Biochimica et Biophysica Acta 1797 (2010) 487–493

Contents lists available at ScienceDirect

Biochimica et Biophysica Acta

journal homepage: www.elsevier.com/locate/bbabio

Conversion of the $g=4.1$ EPR signal to the multiline conformation during the S_2 to S_3 transition of the oxygen evolving complex of Photosystem II

Maria Chrysina, Georgia Zahariou, Nikolaos Ioannidis *, Vasili Petrouleas *

Institute of Materials Science, NCSR "Demokritos", Athens 15310, Greece

ARTICLE INFO

Article history:
Received 13 November 2009
Received in revised form 5 January 2010
Accepted 11 January 2010
Available online 18 January 2010

Keywords:
Photosystem II
EPR
Mn cluster
$g=4.1$
Multiline
Tyrosine Z

ABSTRACT

The oxygen evolving complex of Photosystem II undergoes four light-induced oxidation transitions, S_0–S_1,..., S_3–$(S_4)S_0$ during its catalytic cycle. The oxidizing equivalents are stored at a $(Mn)_4Ca$ cluster, the site of water oxidation. EPR spectroscopy has yielded valuable information on the S states. S_2 shows a notable heterogeneity with two spectral forms; a $g=2$ ($S=1/2$) multiline, and a $g=4.1$ ($S=5/2$) signal. These oscillate in parallel during the period-four cycle. Cyanobacteria show only the multiline signal, but upon advancement to S_3 they exhibit the same characteristic $g=10$ ($S=3$) absorption with plant preparations, implying that this latter signal results from the multiline configuration. The fate of the $g=4.1$ conformation during advancement to S_3 is accordingly unknown. We searched for light-induced transient changes in the EPR spectra at temperatures below and above the half-inhibition temperature for the S_2 to S_3 transition (ca 230 K). We observed that, above about 220 K the $g=4.1$ signal converts to a multiline form prior to advancement to S_3. We cannot exclude that the conversion results from visible-light excitation of the Mn cluster itself. The fact however, that the conversion coincides with the onset of the S_2 to S_3 transition, suggests that it is triggered by the charge-separation process, possibly the oxidation of tyr Z and the accompanying proton relocations. It therefore appears that a configuration of $(Mn)_4Ca$ with a low-spin ground state advances to S_3.

1. Introduction

Photosystem II (PS II) of higher plants, algae and cyanobacteria catalyzes the light-driven oxidation of water to molecular oxygen. Absorption of a photon leads to oxidation of the accessory chlorophyll Chl_{D1} [1–3] and electron transfer to the acceptor side iron–quinone complex, $Q_AFe^{2+}Q_B$ (see 4,5 for recent reviews) via a pheophytin cofactor. Q_A and Q_B are both plastoquinone molecules. Q_A is a one-electron acceptor, while Q_B acts as a two-electron and two-proton acceptor. The positive charge on Chl_{D1} is transferred rapidly to the special pair chlorophyll P_{680} resulting in the formation of P_{680}^+ [6,7]. The latter, in its turn oxidizes a nearby tyrosine residue, tyr Z, to the neutral radical tyr Z$^\bullet$. The final electron donor is a Mn_4Ca cluster, the site of water oxidation, which is oxidized directly by tyr Z$^\bullet$. Four sequential photon-induced charge-separation events lead to the accumulation of four oxidizing equivalents at the Mn cluster. Therefore, the oxygen evolving complex (OEC) of PSII undergoes periodically four one-electron oxidation steps, S_0–S_1,...,S_3–$(S_4)S_0$ (S-state transitions), accompanied by the progressive removal of four protons from two substrate water molecules. Oxygen evolution occurs during the S_3 to $(S_4)S_0$ transition, with the S_4 being a transient state [8–14].

The dark-resting state of the OEC is S_1. The higher S states can be populated and trapped for experimental study by an appropriate number of single turnover flashes of light at elevated temperatures, followed by rapid freezing to cryogenic temperatures. The S-state transitions have half-inhibition temperatures in the vicinity of 230 K, with the exception of the S_1 to S_2 step, which has a half-inhibition temperature of about 135–140 K [15]. Actually S_2 can be partially populated by illumination at 77 K (unpublished results). Temperature limitations are in addition set by the acceptor side. Q_A is an efficient electron acceptor down to liquid helium temperatures, but the electron transfers from Q_A^- to Q_B and from Q_A^- to Q_B^- have half-inhibition temperatures of about 245 K (−28 °C) and 215 K (−58 °C), respectively [16,17].

The S_2 to S_3 step exhibits the highest activation [18] and reorganization energy [19] of all S-state transitions. X-ray absorption spectroscopy suggests the formation of a new 2.7 Å Mn···Mn distance [20], or the inequivalent lengthening of two 2.7 Å Mn···Mn distances to 2.8 and 3.0 Å [21]. XAS data obtained from *T. elongatus* samples in

Abbreviations: PSII, Photosystem II; OEC, oxygen evolving complex; S states, S_0,...,S_4 oxidation states of the OEC; tyr Z or Y_Z, tyrosine 161 of the D2 protein; tyr D or Y_D, tyrosine 160 of the D1 protein; P_{680}, the primary electron donor in PSII; Signal II, the EPR signal of $Y_D^\bullet$; Metalloradical or split signals, EPR signals in the g 2 region attributed to the broadening of the tyr Z$^\bullet$ spectrum by a weak magnetic interaction with the Mn cluster; Q_A, Q_B, the primary, secondary plastoquinone electron acceptors of PSII; MES, 2-[N-Morpholineethanesulfonic acid]; chl, chlorophyll; DCBQ, di-chloro-*p*-benzoquinone; PpBQ, phenyl-*p*-benzoquinone; Duroquinone, tetramethyl benzoquinone; NIR light, near infrared light; EPR, electron paramagnetic resonance

* Corresponding authors. V. Petrouleas is to be contacted at tel.: +30 2106503344; fax: +30 2106519430. N. Ioannidis, tel.: +30 2106503312; fax: +30 2106519430.
E-mail addresses: nioannid@ims.demokritos.gr (N. Ioannidis), vpetr@ims.demokritos.gr (V. Petrouleas).

0005-2728/$ – see front matter © 2010 Elsevier B.V. All rights reserved.
doi:10.1016/j.bbabio.2010.01.008

which Ca^{2+} is substituted by Sr^{2+} indicate a decrease in the two Mn··Ca distances, in the S_3 state [22]. This structural reorganization in S_3 has been proposed earlier, based on the higher binding affinity of calcium in this state [23] and the surprising inertness of the S_3 state towards certain exogenous reductants [24,25].

EPR spectroscopy has yielded a wealth of information on the OEC and the various S states. S_2 is by far the most extensively studied state. Not only its EPR signature is pronounced, but S_2 can be stably produced with close to 100% yield by illumination at cryogenic temperatures. Notable in S_2 is a heterogeneity, which gives rise to two EPR spectral forms; a multiline signal at $g=2$ arising from an $S=1/2$ spin state [26], and a $g=4.1$ signal arising from an $S=5/2$ spin configuration [27]. Both forms oscillate in parallel during the S-state period-four cycle [28]. X-ray absorption spectroscopy studies suggest that the distance between two di-μ-oxo bridged Mn ions of the cluster is longer in the $g=4.1$ compared to the multiline configuration (2.84 Å compared to 2.73 Å) [29]. It is proposed that both signals arise from the 1Mn(III)3Mn(IV) oxidation state configuration of the Mn_4 cluster, but in different conformations of the Mn cluster, which result in modifications of the exchange interactions within the cluster [30,31]. Cyanobacteria (untreated preparations) don't show the $g=4.1$ form [32]. The S_3 state being an integer spin state is more difficult to probe, but it is characterized by broad bimodal signals at around $g=10$ and ~4 in perpendicular mode [33,34], and respective Q-band resonances [35], and several other smaller signals detected recently [36] all attributed to an $S=3$ spin configuration [35,36]. The signals are similar in plant and cyanobacterial PSII preparations, implying that they result from oxidation of the multiline configuration of S_2. No evidence for heterogeneity in S_3 has been reported so far. A number of transient isoelectronic configurations can be however obtained by NIR and visible excitation at liquid helium temperatures [34,37–39] a property that parallels the NIR-induced conversion of the S_2 multiline form to higher spin-state forms [40]. The question, which arises then is, what is the fate of the $g=4.1$ conformation of S_2 upon advancement to S_3. If the heterogeneity of S_2 is preserved in S_3 (that would imply that $g=4.1$ advances to an EPR-silent conformation), then two apparently different conformations of the Mn core of the OEC are equally efficient in performing the specialized water-splitting chemistry.

In the present paper we have searched for transient changes in the EPR spectra of the Mn_4O_xCa complex during the S_2 to S_3 transition at temperatures below and above the half-inhibition temperature for this transition, which is approx. 230 K [15]. Short-lived transients should live longer near the half-inhibition temperature. We present evidence that the $g=4.1$ ($S=5/2$) configuration of S_2 converts to an $S=1/2$ multiline form prior to advancement to S_3.

2. Materials and methods

2.1. PSII sample isolation

PSII-enriched thylakoid membranes were isolated from spinach following standard methods [41,42]. Samples for EPR measurements were suspended in 0.4 M sucrose, 15 mM NaCl, 40 mM MES–NaOH, pH 6.5, at about 6–8 mg chl/mL and stored in liquid nitrogen until use. All samples prior to the EPR experiments were given a pre-flash at 265 K and were subsequently dark adapted for 30–40 min at 0–4 °C. This poises all centers to the S_1 state. Samples were subsequently supplemented with 1 mM of either di-chloro-*p*-benzoquinone (DCBQ), or phenyl-*p*-benzoquinone (PpBQ), or tetramethyl-*p*-benzoquinone (duroquinone), all dissolved in dimethyl sulfoxide, as exogenous electron acceptors.

2.2. Preparation of samples in the $S_2…Q_A$ state

The starting state, $S_2…Q_A$, in the experiments of Figs. 2 and 3 of the main paper and the three figures of the Supplementary data was produced by either of the following two procedures: two cycles of 4 min continuous illumination at 190 K, followed by incubation at ca. 265 K for 30 s (or incubation at somewhat lower temperatures for 1 to 2 min) to allow for electron transfer from Q_A^- to the exogenous quinone. Single-saturating flash illumination at temperatures in the range of 190 K to 265 K, again was followed by incubation at 265 K for 30 s. In order to minimize the fraction of misses, an additional illumination at 190 K was given in the latter case followed by incubation at 265 K. This protocol in combination with the pre-flash (see previous paragraph) ensured that no significant fraction of centers remained in S_1. Other illumination conditions are described in the specific experiments. We have been alerted by the possibility of the NIR conversion of the multiline to the $g=4.1$ form during illumination at 200 K [40]. Typically, whenever 200 K illumination was employed in the S_2 state, the sample was allowed to equilibrate at 243 K or higher temperatures (up to 265 K) for 1 min or 30 s. Therefore the starting S_2 spectra in the various experiments represent the equilibrium $S_2…Q_A$ configuration.

2.3. Illumination conditions

A studio photographic flash unit, Elinchrom Style RX 1200, with a variable flash power up to 1200 W, and pulse duration (half width at half height) of 1–2 ms was used for flash excitation of the samples. The unit was equipped with a flexible fiber light extension for illumination inside the cavity. In many of the present experiments immediate cooling of the sample for EPR measurements at 10 K was necessary. The sample was accordingly flash illuminated inside an appropriate acetone bath, and then rapidly wiped and transferred to a liquid nitrogen bath and from there to the EPR cryostat at 10 K. In certain experiments a more rapid cooling procedure was employed. The sample after equilibration at the appropriate temperature in the acetone bath, was wiped and then placed over a liquid nitrogen dewar for the flash and rapid cooling. In this latter procedure a higher uncertainty exists on the exact temperature of the sample during the illumination.

2.4. Quantification of the S_3 state

The S_3 state was approximately quantified by comparison of the size of the characteristic signal at $g=10$ with earlier spectra (after appropriate normalization of their S_2 state signals) obtained from samples in which the S_3 to S_0 transition was inhibited by the presence of atrazine [34].

2.5. EPR measurements

EPR measurements were obtained with an extensively upgraded Bruker ER-200D spectrometer interfaced to a personal computer and equipped with an Oxford ESR 900 cryostat, an Anritsu MF76A frequency counter and a Bruker 035M NMR gaussmeter. The Signal-Channel unit was replaced with an SR830 digital lock-in amplifier by Stanford Research. The perpendicular 4102ST cavity was used, and the microwave frequency was 9.41 GHz.

3. Results

3.1. Efficiency of the S-state transitions in the temperature range 220–273 K

The period-four oscillation of the EPR spectra of the OEC is commonly studied by flash excitation at temperatures above 0 °C. The S-state cycle should however, proceed efficiently below 0 °C (273 K), as long as the temperature is higher than the half-inhibition temperature for S-state advancement (approx. 230 K for all except ca. 135 K or even lower for the S_1 to S_2 step [15]). Additional

limitations are set by the acceptor side with half-inhibition temperatures of about 245 K and 215 K for Q_A^- to Q_B and Q_A^- to Q_B^- electron transfer [16,17] respectively while the reduction of Q_A is activationless down to 4.2 K. The above limitations may vary somewhat in different PSII preparations. The use in particular of excess concentrations of exogenous quinones and/or the fact that some of these quinones oxidize the non-heme iron [43,44] may lower the half-inhibition temperatures for oxidation of Q_A^-. The present paper is centered on the S_2 to S_3 transition at temperatures near (below or above) 230 K. As a test of the behavior of the PSII material used and the adequacy of our illumination set-up to induce single turnovers in this temperature range, we have examined first the efficiency of S-state turnover in the temperature range 220–273 K.

EPR studies of period-four oscillations below 273 K are very rare or non-published, despite the fact that the various transitions are expected to be slower and the demand on expensive powerful sub-μs light sources can be relaxed. Furthermore, since the sample is never thawed throughout the cycle, the risk of damage is minimized and a single sample can be progressively excited through the S-state cycle. We have found that reasonable period-four oscillations of the EPR spectra can be achieved at temperatures below 0 °C by using a very simple illumination set-up/procedure: a flash-light source such as the ones used in commercial photography with a flash length of 1–2 ms, and cycling of the same sample through the various S states. Furthermore, since the length of the flash is long, the flashes are saturating even for the densest EPR samples. Accordingly, no dilution of the samples is necessary and no compromise is made with respect to the signal to noise.

Fig. 1 shows the variation of the EPR spectra during sequential flash illumination at representative temperatures below 273 K. At 261 K (panel A) the oscillations are reasonably good. Not only the multiline and $g=4.1$ signals oscillate in concert, but also the $g=10$ signal of the S_3 state shows oscillations with maxima on the 2nd and 6th flash. Similar behavior was observed at about 243 K (data not shown) indicating that the half-inhibition temperature for the Q_A^- to Q_B electron transfer is lower than 245 K in the presence of excess concentrations of exogenous quinone. At 233 K (panel B), a temperature that is near the half-inhibition temperature for the S_2 to S_3 transition, the second flash produces only ca 20% of S_3 (compared with approx. 50% in the experiment of panel A), and therefore oscillations cannot proceed. At 226 K (panel B) the misses for the same transition become even higher, and only a small fraction of S_3 (ca 10%) is produced. It should be noted that the experiments of panel (B) are not limited by the Q_A^-/Q_B electron transfer since the starting state on the second flash is $S_2\ldots Q_A$. No discernible amounts of S_3 could be produced in similar experiments at 210 K or lower (data not shown). It should be noted however, that the S_2 to S_3 transition can be activated by illumination at temperatures well below the half-inhibition temperature and rapid transfer above the half-inhibition temperature [45].

An unusual observation in the experiments of Fig. 1 panel (B) is that the decrease of the $g=4.1$ and multiline signals after the 2nd flash is unequal. This is more pronounced in the experiment at 226 K. The $g=4.1$ decreases by more than 25%, while the multiline signal remains practically unchanged. We look more closely on this effect below.

3.2. Changes in the EPR spectra during the S_2 to S_3 advancement

Fig. 2 panel (A) shows the sequential spectral changes observed in the $S_2\ldots Q_A$ state when the latter is subjected to flashes of light at temperatures in the vicinity of the half-inhibition temperature for the S_2 to S_3 transition. The first spectrum represents the $S_2\ldots Q_A$ state. The following spectra represent the changes induced by single flashes of light given at the indicated temperatures. Prior to each flash the sample was equilibrated at the respective temperature for 1 min.

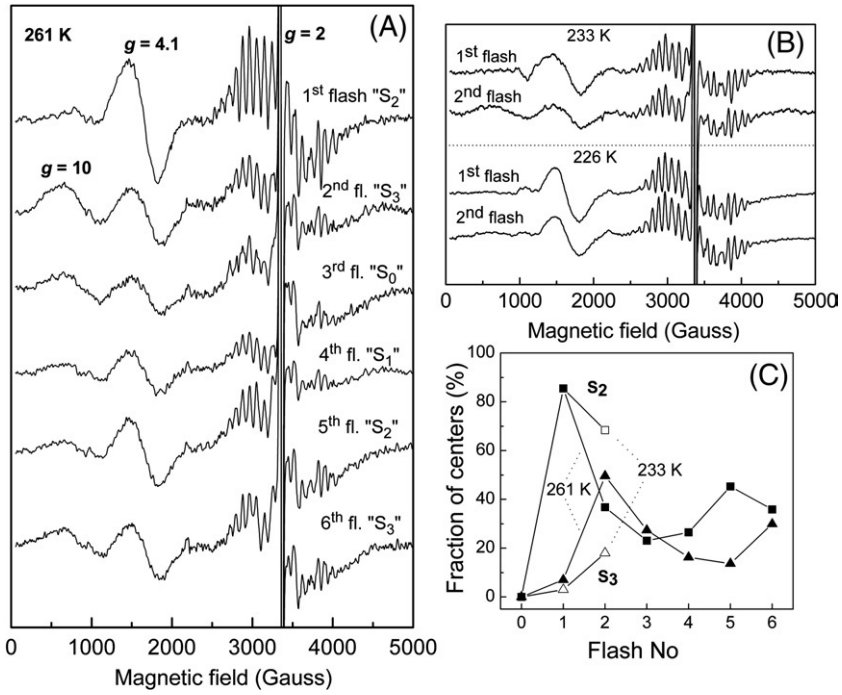

Fig. 1. Panel (A): Representative EPR spectra depicting oscillations at about −12 °C (261 K) in a sample supplemented with 1 mM DCBQ. The spectrum of the initial dark adapted S_1 state was subtracted from all spectra shown. The sample received each flash at 261 K, followed by rapid cooling to liquid helium temperatures to record the EPR spectrum. Prior to the next flash, the sample was incubated at 261 K in the dark, for 1 min, in order to allow for electron transfer from Q_A^- to the exogenous quinone. Panel (B): The effect of two flash cycles at 233 K (upper), and 226 K (lower). The samples, after the first flash, were incubated at 265 K for 30 s to allow for electron transfer from Q_A^- to the exogenous quinone. Panel (C): Oscillation patterns of the S_2 signal (squares represent the average of the multiline and the $g=4.1$ intensity) and the S_3 $g=10$ signal (triangles) calculated from the spectra in panels (A) (filled symbols) and (B) (open symbols). EPR conditions: microwave frequency 9.41 GHz, modulation frequency 100 KHz, modulation amplitude 25 Gpp, microwave power 32 mW, and temperature 10 K.

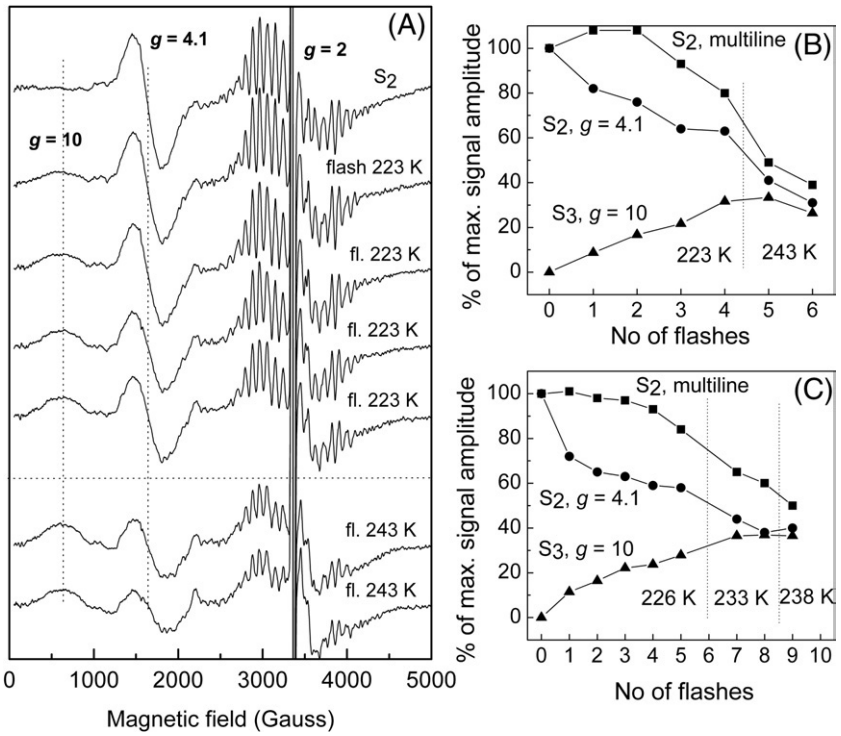

Fig. 2. Panel (A): Spectral changes induced by flash illumination of the $S_2...Q_A$ state near the half-inhibition temperature for the S_2 to S_3 transition. The spectrum of the initial dark adapted S_1 state was subtracted from all spectra shown. The first spectrum represents the $S_2...Q_A$ state prepared as described in the Materials and methods. Subsequent traces were recorded immediately (approx. 2 s cooling time to 77 K after each flash) after flash illumination at the indicated temperatures. Prior to each flash the sample was incubated for 1 min at the temperature of the flash. Panel (B): Variation (%) of the amplitude of signals shown in panel (A), with the number of flashes administered. Panel (C): Similar experiment to panels (A) and (B), but in a somewhat different temperature range. EPR conditions as in Fig. 1.

After the flash, the sample was cooled immediately (within a few seconds) to 77 K and from there to 10 K for the recording of the EPR spectrum. The initial sequence of four flashes at 223 K was followed by flashes at 243 K. Panel (B) plots the evolution of the various signals in the spectra of panel (A). Panel (C) is a plot from a similar experiment, but in a somewhat different temperature range.

An overall decay of the S_2 signals is observed in Fig. 2, accompanied by a parallel evolution of the characteristic EPR signal of S_3 at $g=10$ [32,34]. At 223–226 K S_3 cannot advance further, because the temperature is too low for secondary electron transfer from Q_A^- to Q_B [16,17]. The spectra are therefore dominated by the S_2 and S_3 states. At higher temperatures, S_3 declines after reaching a maximum, indicating that the secondary electron transfer has been activated and advancement to S_0 occurs. Accurate quantitation of the fraction of centers represented by each signal is not easy, but this is of secondary importance in the present paper.

A striking observation in Fig. 2 is that, the $g=4.1$ configuration of S_2 decays much faster than the multiline throughout the temperature range examined. The difference is largest at 223–226 K, but a significant deviation exists even at 233 K, while the decaying fractions converge above about 240 K. The multiline in the experiment of panels (A) and (B) increases slightly during the first two flashes before it starts decaying. If it wasn't for the transient increase in the intensity of the multiline one might assume, that the $g=4.1$ S_2 configuration advances more efficiently to S_3, while the S_2-multiline to S_3 transition is partially constrained. The transient increase of the multiline and the following experiments suggest however, a different explanation.

3.3. Reversible conversion of the $g=4.1$ to the multiline conformation

We have looked more closely into the changes in the $g=4.1$ and multiline signals following flash excitation at 223 K. Fig. 3 examines the variation of the $g=4.1$ and multiline S_2 state signals following a flash of light at 223 K and subsequent dark incubation at different temperatures. A faster procedure for cooling the sample after the flash was employed in this experiment (see Materials and methods). The spectra during the sequential treatments are shown in panel (A) while the variation in the intensity of the signals is plotted in panel (B).

Clearly the $g=4.1$ signal decreases substantially after the flash at 223 K, and this is accompanied by an increase of the multiline signal. This change is not reversed during the subsequent few-min incubation at 190 K and 223 K (treatments (c) and (d) in Fig. 3 panels (A) and (B)). Incubation at 243 K (treatment (e)) restores, however, the initial intensity of both signals, albeit at a slightly diminished level, presumably due to a partial (ca 5%) advancement to S_3. It is notable, that a new flash at 223 K (trace (f)) induces again similar changes to the spectra with the first flash.

3.4. Trapping of $S_2Y_Z^{\bullet}$

By taking the difference between traces b and d, (Fig. 3A) a split signal at $g=2$ can be observed. The signal has been recorded under higher resolution conditions in panel (C) (continuous trace) where it is compared with the spectrum of $S_2Y_Z^{\bullet}$ (dashed trace). The latter was trapped by a flash illumination at 190 K of a separate sample prepared in the $S_2...Q_A$ state [45]. The relative scaling of the two spectra is arbitrary. Clearly, the two spectra in panel (C) have a very similar structure (except for variations in the middle, which are due to car^+ or chl^+ radicals). We therefore tentatively assign the present split signal to $S_2Y_Z^{\bullet}$, but a more detailed justification will be presented elsewhere. Therefore tyr $Z^{\bullet}$ can be trapped by a flash illumination at 223 K, but as has been estimated by comparison with the unsaturated spectrum of tyr $D^{\bullet}$, the signal trapped in the present experiment does not represent more than a few percent of centers. Based on our earlier experiments, the recombination time of this intermediate at 223 K is

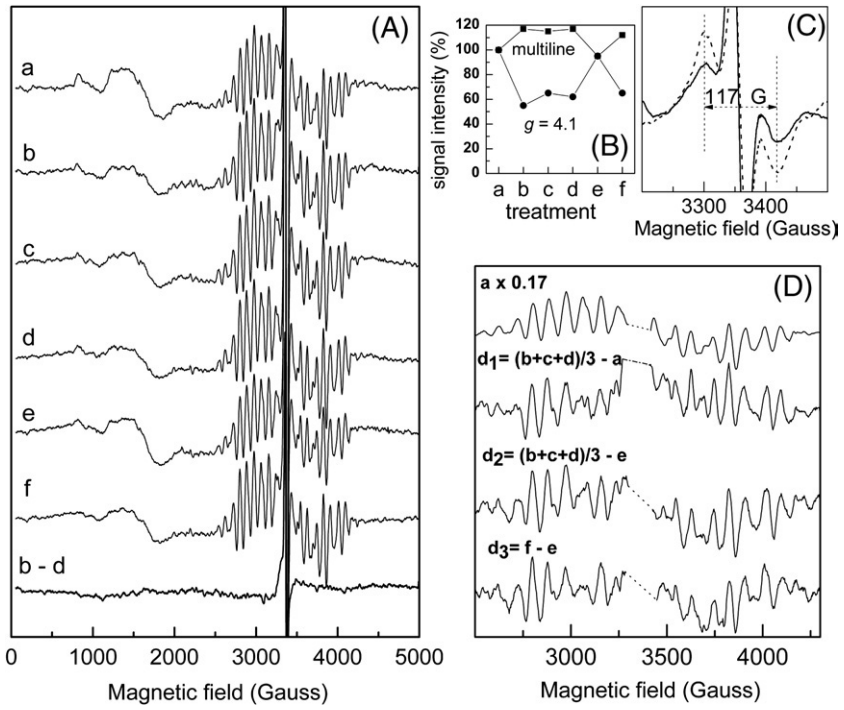

Fig. 3. Reversible conversion of the $g=4.1$ to the multiline configuration. The spectrum of the initial dark adapted S_1 state was subtracted from all spectra shown. Panel (A): (a) Spectrum of the $S_2...Q_A$ state. Subsequently the sample received the following sequential treatments. (b) Flash illumination at 223 K followed by rapid cooling to liquid helium temperatures. (c) Dark incubation at 190 K for 4 min, followed in (d) by 3 min at 223 K, and in (e) by 2 min at 243 K. (f) New flash illumination at 223 K and rapid cooling. The last trace is the difference between traces (b) and (d). Panel (B): Percent variation of the intensity of the multiline (squares) and $g=4.1$ (circles) signals during the corresponding treatments in panel (A). Panel (C): Continuous trace: Difference of narrow scan traces recorded after treatments (b) and (d) in panel A. Dashed trace: Reference spectrum of the $S_2Y_Z^{\bullet}$ signal (45). Panel (D): Difference spectra (d_1, d_2, and d_3) of the average of traces (b), (c), (d) minus traces (a) or (e), and (f) minus (e), as indicated, compared with spectrum (a) appropriately normalized. The central region of the spectra was omitted for clarity. The sample was supplemented with 1 mM DCBQ. EPR conditions: as in Fig. 1, except for the microwave power which was100 mW in panel (C).

in the sub-s range for the majority of centers, while a minority fraction decays with a halftime in the order of a few seconds [46]. This explains why only a small fraction of the $S_2Y_Z^{\bullet}$ signal is trapped in Fig. 3(C) by our cooling protocol which is limited to cooling times of 1 to 2 s. Apparently tyr $Z^{\bullet}$ decays much faster than the alterations in the $g=4.1$ and multiline spectra.

3.5. Lineshapes of the multiline signal

In the last trace of Fig. 3, panel (A) we chose to present the difference between traces (b) and (d), which have matching intensities of the multiline signal, in order to obtain a clear spectrum of the $S_2Y_Z^{\bullet}$ transient. In panel (D) we examine the lineshape of the multiline signal that is added to the normal S_2 multiline spectrum by the light-induced conversion of the $g=4.1$ signal to the multiline form. The panel compares the difference of the average of traces (b), (c), (d) minus traces (a) and (e), and the difference of trace (f) minus (e) with spectrum (a) appropriately normalized. The latter is a typical multiline pattern similar to what is observed e.g. by illumination at 200 K. For reasons of simplicity and improvement of signal to noise the average of the differences is presented, as indicated. Traces d_1, d_2, and d_3 are all similar, but show notable differences from spectrum (a). The main difference is in the outer multiline peaks which are more intense in the former. Actually, the traces d_1, d_2, and d_3 show striking similarities to a heterogeneous multiline form presented by Boussac [47]. This form represents the population of centers in S_2 that convert reversibly to the $g=4.1$ form upon NIR illumination at temperatures below about 200 K. In the present case the traces d_1, d_2, and d_3 represent the multiline signal that develops reversibly at the expense of the $g=4.1$ signal by visible illumination at ca 223 K.

4. Discussion

The present data indicate conversion of the S_2 $g=4.1$ ($S=5/2$) to a multiline ($S=½$) conformation during the light-induced advancement to S_3. It therefore appears that the heterogeneity of the lower S states is not transmitted to the highest S states, and the OEC at the critical last steps of its catalytic function is homogeneous. A configuration of the Mn cluster with a low-spin ground state advances to S_3. This observation is not inconsistent with the fact that both the multiline and the $g=4.1$ conformations oscillate in parallel during the period-four water-splitting cycle of the OEC [28]. Both signals are observed only in S_2. During a period-four oscillation cycle the heterogeneity is presumably restored upon population of the lower S states, S_0 or S_1 (evidence that the heterogeneity of S_2 is also present in S_1 has been presented in [48]). The decay of S_3 on the other hand produces proportional amounts of the two conformations of S_2. It is expected that the decay of S_3 would produce transiently higher amounts of the multiline conformation. This is, however difficult to detect because the decay rate of S_3 at any temperature appears to be lower than the time needed for the equilibration of the two S_2 conformations (for an example of a study of the S_3 decay at 243 K see [49]). Another factor that would complicate things is the faster decay of the $g=4.1$ compared to the multiline signal [28].

4.1. The driving force for the $g=4.1$ to the multiline conversion

Boussac [47] has shown that a heterogeneous population of S_2 characterized by a modified multiline spectrum with stronger outer peaks exists as part of the commonly observed multiline spectrum in certain types of PSII preparations. This upon NIR excitation at

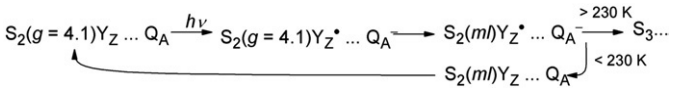

Scheme 1. Postulated reversible conversion of the $g=4.1$ to the multiline conformation, driven by the oxidation of tyr Z during the S_2 to S_3 transition (ml stands for multiline).

temperatures below 200 K converts to the $g=4.1$ signal. In the present case the reverse effect, conversion of the $g=4.1$ signal to the modified multiline signal, is induced by visible-light illumination. It might be argued that this observation reveals a new light sensitivity of the Mn cluster in the visible region of the spectrum. We cannot at present exclude this possibility, but the fact that the new conversion occurs at temperatures near and above the onset of the S_2 to S_3 transition suggests that the transition is driven by the charge-separation process. Additional evidence in support of this assignment is provided by earlier experiments with acetate inhibited samples.

Acetate treatment converts the entire S_2 population to the $g=4.1$ form. In addition, it blocks advancement to the S_3 state. Formation of the $S_2Y_Z^{\bullet}$ terminal state in such samples is accompanied by conversion of the $g=4.1$ to the multiline signal (see e.g. [50,51]). A correlation exists between the decay of the $Y_Z^{\bullet}$ split radical signal, the multiline signal that accompanies it and the recovery of the $g=4.1$ signal during storage at 200 K [51]. On the other hand, the multiline persists even after elimination of the tyr $Z^{\bullet}$ radical by NO, indicating that it is not the magnetic interaction between the radical and the Mn that drives the conversion. The effect of the magnetic interaction is a slight shift of the multiline peaks. In the present experiments, too, the $g=4.1$ to the multiline change persists after decay of the tyr $Z^{\bullet}$ radical, Fig. 3. The $g=4.1$ conversion is more limited in the present case, but this must be due to the lower temperature of illumination, 223 K compared to >273 K in the case of acetate. It is not possible of course to trace the respective changes in the untreated samples at 273 K or higher, because above about 230 K $S_2Y_Z^{\bullet}$ advances rapidly to S_3.

The driving force for the $g=4.1$ to multiline conversion is, most likely, the oxidation of tyr Z and the accompanying hydrogen bonding changes, as has been assumed for the acetate treated samples [51]. Scheme 1 describes the sequential changes that may be occurring in the fraction of centers that are characterized by the $g=4.1$ signal. The scheme applies to acetate treated samples, as well, with the exception that the S_2 to S_3 transition is blocked in this case.

The fact that an intimate relationship exists between tyr Z and the Mn cluster is supported by several pieces of evidence (for a critical discussion see [52], also [45]), which suggest that changes in the charge at the Mn site affect the *pK* of the base partner of tyr Z (His 190) and vice versa. One of the consequences is that, oxidation of tyr Z in S_0 and S_1 is possible down to liquid helium temperatures, while oxidation of tyr Z in the more positively charged S_2 state is constrained to temperatures higher than 77 K [45]. It is likely that the proton movements occurring during tyr Z oxidation in the latter case affect the conformation of the Mn cluster, imposing conversion of the $g=4.1$ to the multiline configuration. The reduction of tyr $Z^{\bullet}$ is not necessarily accompanied by immediate restoration of the charge equilibria in the Mn cluster (this may be limited by a thermal activation barrier), and this explains why the reverse conversion of the multiline to the $g=4.1$ signal occurs with a delay in Fig. 3.

While the above considerations provide a plausible explanation of the observed conversion of the $g=4.1$ to the multiline form, it should be noted that the $S_2(g=4.1)Y_Z^{\bullet}$ intermediate shown in Scheme 1 has not been detected so far, in either the acetate treated or the untreated samples. The trapping of the 117 G split signal, assigned to $S_2Y_Z^{\bullet}$ in untreated samples [47], was linked to the multiline configuration of S_2, as its formation was coupled to magnetic perturbation of the multiline spectrum. It is possible, that the $S_2(g=4.1)Y_Z^{\bullet}$ intermediate is broader and more difficult to detect, or is constrained at temperatures lower than about 223 K and proceeds to the next step much faster than the time resolution of the experiments.

5. Conclusions

The heterogeneity of the S_2 state signals is not a universal property of the PSII samples. Cyanobacterial PSII preparations are characterized by the multiline configuration only. The present results suggest that even in BBY spinach preparations exhibiting a prominent $g=4.1$ signal (representing close to 50% of the centers) a uniform configuration of S_2, the one exhibiting the multiline signal, proceeds to S_3. The present findings suggest accordingly that at the most critical stages of the oxygen evolution process the Mn cluster acts in a homogeneous conformation. At the current resolution of the OEC structure a multitude of the Mn cluster conformations fulfill the experimental criteria (see e.g. [31]). To the extent that such fine details, as the ground state spin configuration of the Mn cluster, can be utilized to screen out inappropriate Mn conformations, the present results suggest that only the conformations favoring an $S=1/2$ ground state in S_2 would be viable for performing the water-splitting chemistry.

Appendix A. Supplementary data

Supplementary data associated with this article can be found, in the online version, at doi:10.1016/j.bbabio.2010.01.008.

References

[1] B.A. Diner, E. Schlodder, P.J. Nixon, W.J. Coleman, F. Rappaport, J. Lavergne, W.F. Vermaas, D.A. Chisholm, Site-directed mutations at D1-His198 and D2-His97 of photosystem II in synechocystis PCC 6803: sites of primary charge separation and cation and triplet stabilization, Biochemistry 40 (2001) 9265–9281.
[2] M.L. Groot, N.P. Pawlowicz, L.J. van Wilderen, J. Breton, I.H. van Stokkum, R. van Grondelle, Initial electron donor and acceptor in isolated Photosystem II reaction centers identified with femtosecond mid-IR spectroscopy, Proc. Natl. Acad. Sci. U. S. A. 102 (2005) 13087–13092.
[3] A.R. Holzwarth, M.G. Muller, M. Reus, M. Nowaczyk, J. Sander, M. Rögner, Kinetics and mechanism of electron transfer in intact photosystem II and in the isolated reaction center: pheophytin is the primary electron acceptor, Proc. Natl. Acad. Sci. U.S. A. 103 (2006) 6895–6900.
[4] B.A. Diner, G.T. Babcock, Structure, dynamics, and energy conversion efficiency in photosystem II, in: D.R. Ort, C.F. Yocum (Eds.), Oxygenic Photosynthesis: the Light Reactions, Kluwer, Dordrecht, 1996, pp. 213–247.
[5] V. Petrouleas, A.R. Crofts, The iron–quinone acceptor complex, in: T. Wydrzynski, K. Satoh (Eds.), Photosystem II: The Water/Plastoquinone Oxido-reductase in Photosynthesis, Kluwer Academic Publishers, Dordrecht, The Netherlands, 2005, pp. 177–206.
[6] F. Rappaport, B.A. Diner, Primary photochemistry and energetics leading to the oxidation of the (Mn)4Ca cluster and to the evolution of molecular oxygen in Photosystem II, Coord. Chem. Rev. 252 (2007) 259–272.
[7] G. Renger, I.I. Photosystem, Structure and mechanism of the water–plastoquinone oxidoreductase, Photosynth. Res. 92 (2007) 407–425.
[8] C. Goussias, A. Boussac, A.W. Rutherford, Photosystem II and photosynthetic oxidation of water: an overview, Philos. Trans. R. Soc. London, Ser. B 357 (2002) 1369–1381.
[9] T.G. Carrell, A.M. Tyryskin, G.C. Dismukes, An evaluation of structural models for the photosynthetic water-oxidizing complex derived from spectroscopic and X-ray diffraction signatures, J. Biol. Inorg. Chem. 7 (2002) 2–22.
[10] R.D. Britt, K.A. Campbell, J.M. Peloquin, M.L. Gilchrist, C.P. Aznar, M.M. Dicus, J. Robblee, J. Messinger, Recent pulsed EPR studies of the Photosystem II oxygen-evolving complex: implications as to water oxidation mechanisms, Biochim. Biophys. Acta 1655 (2004) 158–171.
[11] V.K. Yachandra, The catalytic manganese cluster: organization of the metal ions, in: T. Wydrzynki, K. Satoh (Eds.), Photosystem II: the Water/Plastoquinone Oxido-reductase of Photosynthesis, Kluwer Academic Publishers, Dordrecht, The Netherlands, 2005, pp. 235–260.
[12] W. Hillier, J. Messinger, Mechanisms of photosynthetic oxygen production, in: T. Wydrzynki, K. Satoh (Eds.), Photosystem II: The Water/Plastoquinone Oxido-reductase of Photosynthesis, Kluwer Academic Publishers, Dordrecht, The Netherlands, 2005, pp. 567–608.
[13] J.P. McEvoy, G.W. Brudvig, Water-splitting chemistry of photosystem II, Chem. Rev. 106 (2006) 4455–4483.

[14] T.J. Meyer, M.H.V. Huynh, H.H. Thorp, The possible role of proton-coupled electron transfer (PCET) in water oxidation by photosystem II, Angew. Chem. Int. Ed. 46 (2007) 5284–5304.
[15] S. Styring, A.W. Rutherford, Deactivation kinetics and temperature-dependence of the S-state transitions in the oxygen-evolving system of Photosystem-II measured by electron paramagnetic resonance spectroscopy, Biochim. Biophys. Acta 933 (1988) 378–387.
[16] F. Reifarth, G. Renger, Indirect evidence for structural changes coupled with Q_B^- formation in photosystem II, FEBS Lett. 428 (1998) 123–126.
[17] Chr. Fufezan, Ch. Zhang, A. Krieger-Liszkay, W. Rutherford, Secondary quinone in Photosystem II of *Thermosynechococcus elongatus*: semiquinone–iron EPR signals and temperature dependence of electron transfer, Biochemistry 44 (2005) 12780–12789.
[18] M. Karge, K.D. Irrgang, G. Renger, Analysis of the reaction coordinate of photosynthetic water oxidation by kinetic measurements of 355 nm absorption changes at different temperatures in Photosystem II preparations suspended in either H_2O or D_2O, Biochemistry 36 (1997) 8904–8913.
[19] G. Renger, G. Christen, M. Karge, H.J. Eckert, K.D. Irrgang, Application of the Marcus theory for analysis of the temperature dependence of the reactions leading to photosynthetic water oxidation: results and implications, J. Biol. Inorg. Chem. 3 (1998) 360–366.
[20] M. Haumann, C. Muller, P. Liebisch, L. Iuzzolino, J. Dittmer, M. Grabolle, T. Neisius, W. Meyer-Klaucke, H. Dau, Structural and oxidation state changes of the Photosystem II manganese complex in four transitions of the water oxidation cycle (S0→S1, S1→S2, S2→S3, and S3, 4→S0) characterized by X-ray absorption spectroscopy at 20 K and room temperature, Biochemistry 44 (2005) 1894–1908.
[21] W.C. Liang, T.A. Roelofs, R.M. Cinco, A. Rompel, M.J. Latimer, W.O. Yu, K. Sauer, M.P. Klein, V.K. Yachandra, Structural change of the Mn cluster during the S_2→S_3 State transition of the oxygen-evolving complex of Photosystem II. Does it reflect the onset of water/substrate oxidation? Determination by Mn X-ray absorption spectroscopy, J. Am. Chem. Soc. 122 (2000) 3399–3412.
[22] Y. Pushkar, J. Yano, K. Sauer, A. Boussac, V.K. Yachandra, Structural changes in the Mn_4Ca cluster and the mechanism of photosynthetic water splitting, Proc. Natl. Acad. Sci. U. S. A. 105 (2008) 1879–1884.
[23] A. Boussac, A.W. Rutherford, Ca^{2+} binding to the oxygen evolving enzyme varies with the redox state of the Mn cluster, FEBS Lett. 236 (1988) 432–436.
[24] J. Messinger, U. Wacker, G. Renger, Unusual low reactivity of the water oxidase in the redox state S3 toward exogenous reductants. Analysis of the NH2OH and NH2NH2 induced modifications of flash induced oxygen evolution in isolated spinach thylakoids, Biochemistry 30 (1991) 7852–7862.
[25] N. Ioannidis, and V. Petrouleas, Interaction of higher S-states of the OEC with reductants. Is the S3 state a radical containing state? Photosynthesis: fundamental aspects to global perspectives. 13th International Congress of Photosynthesis, (2004) 361–362 (A. van der Est, and D. Bruce eds.), CD-ROM edition, Montreal, Canada).
[26] G.A. Lorigan, R.D. Britt, Temperature-dependent pulsed electron paramagnetic resonance studies of the S2 state multiline signal of the photosynthetic oxygen-evolving complex, Biochemistry 33 (1994) 12072–12076.
[27] A. Boussac, A.W. Rutherford, Comparative study of the $g=4.1$ EPR signals in the S_2 state of photosystem II, Biochim. Biophys. Acta 1457 (2000) 145–156.
[28] J.L. Zimmermann, A.W. Rutherford, Electron paramagnetic resonance properties of the S_2 State of the oxygen-evolving complex of Photosystem II, Biochemistry 25 (1986) 4609–4615.
[29] W. Liang, M.J. Latimer, H. Dau, T.A. Roelofs, V.K. Yachandra, K. Sauer, M.P. Klein, Correlation between structure and magnetic spin state of the manganese cluster in the oxygen-evolving complex of photosystem II in the S_2 state: determination by X-ray absorption spectroscopy, Biochemistry 33 (1994) 4923–4932.
[30] J.M. Peloquin, K.A. Campbell, D.W. Randall, M.A. Evanchik, V.L. Pecoraro, W.H. Armstrong, R.D. Britt, ^{55}Mn ENDOR of the S_2-state multiline EPR signal of Photosystem II: implications on the structure of the tetranuclear Mn cluster, J. Am. Chem. Soc. 122 (2000) 10926–10942.
[31] D.A. Pantazis, M. Orio, T. Petrenko, S. Zein, W. Lubitz, J. Messinger, F. Neese, Structure of the oxygen-evolving complex of photosystem II: information on the S_2 state through quantum chemical calculation of its magnetic properties, Phys. Chem. Chem. Phys. 11 (2009) 6788–6798.
[32] A.E. McDermott, V.K. Yachandra, R.D. Guiles, J.L. Cole, S.L. Dexheimer, R.D. Britt, K. Sauer, M.P. Klein, Characterization of the manganese O_2-evolving complex and the iron–quinone acceptor complex in photosystem II from a thermophilic cyanobacterium by electron paramagnetic resonance and X-ray absorption spectroscopy, Biochemistry 27 (1988) 4021–4031.
[33] T. Matsukawa, H. Mino, D. Yoneda, A. Kawamori, Dual-mode EPR study of new signals from the S_3-state of oxygen-evolving complex in photosystem II, Biochemistry 38 (1999) 4072–4077.
[34] N. Ioannidis, V. Petrouleas, Electron paramagnetic resonance signals from the S_3 state of the oxygen-evolving complex. A broadened radical signal induced by low-temperature near infrared light illumination, Biochemistry 39 (2000) 5246–5254.
[35] Y. Sanakis, J. Sarrou, G. Zahariou, V. Petrouleas, Q-band EPR studies of the S_3 state of the OEC of the Photosystem II, Proceedings 14th Congress of Photosynthesis, Glasgow, Scotland, 2007, pp. 481–484.
[36] A. Boussac, M. Sugiura, A.W. Rutherford, P. Dorlet, Complete EPR spectrum of the S_3-state of the oxygen-evolving Photosystem II, J. Am. Chem. Soc. 131 (2009) 5050–5051.
[37] N. Ioannidis, J.H.A. Nugent, V. Petrouleas, Intermediates of the S_3 State of the Oxygen-Evolving Complex of Photosystem II, Biochemistry 41 (2002) 9589–9600.
[38] A. Boussac, M. Sugiura, T.L. Lai, A.W. Rutherford, Low-temperature photochemistry in photosystem II from *Thermosynechococcus elongatus* induced by visible and near-infrared light, Philos. Trans. R. Soc. Lond. B Biol. Sci. 363 (2008) 1203–1210.
[39] K.G.W. Havelius, J.H. Su, Y. Feyziyev, F. Mamedov, S. Styring, Spectral resolution of the split EPR signals induced by illumination at 5 K from the S_1, S_3, and S_0 states in photosystem II, Biochemistry 45 (2006) 9279–9290.
[40] A. Boussac, S. Un, O. Horner, A.W. Rutherford, High-spin states ($S \geq 5/2$) of the Photosystem II manganese complex, Biochemistry 37 (1998) 4001–4007.
[41] D.A. Berthold, G.T. Babcock, C.F. Yocum, A highly resolved, oxygen-evolving photosystem-II preparation from spinach thylakoid membranes — electron-paramagnetic-resonance and electron-transport properties, FEBS Lett. 134 (1981) 231–234.
[42] R.C. Ford, M.C.W. Evans, Isolation of a photosystem-2 preparation from higher-plants with highly enriched oxygen evolution activity, FEBS Lett. 160 (1983) 159–164.
[43] J.L. Zimmerrnann, A.W. Rutherford, Photoreductant-induced oxidation of Fe2+ in the electron acceptor complex of Photosystem II, Biochim. Biophys. Acta 851 (1986) 416–423.
[44] V. Petrouleas, B.A. Diner, Light-induced oxidation of the acceptor-side Fe(II) of Photosystem II by exogenous quinones acting through the Q_B binding site. I. Quinones, kinetics and pH-dependence, Biochim. Biophys. Acta 893 (1987) 126–137.
[45] N. Ioannidis, G. Zahariou, V. Petrouleas, Trapping of the S_2 to S_3 state intermediate of the oxygen-evolving complex of photosystem II, Biochemistry 45 (2006) 6252–6269.
[46] N. Ioannidis, G. Zahariou, V. Petrouleas, The EPR spectrum of tyrosine $Z^{\bullet}$ and its decay kinetics in O_2-evolving photosystem II preparations, Biochemistry 47 (2008) 6292–6300.
[47] A. Boussac, Inhomogeneity of the EPR multiline signal from the S_2-state of the photosystem II oxygen-evolving enzyme, J. Biol. Inorg. Chem. 2 (1997) 580–585.
[48] G. Sioros, D. Koulougliotis, G. Karapanagos, V. Petrouleas, The $S_1Y_z^{\bullet}$ metalloradical EPR signal of Photosystem II contains two distinct components that advance respectively to the multiline and $g=4.1$ conformations of S_2, Biochemistry 46 (2007) 210–217.
[49] N. Ioannidis, V. Petrouleas, Decay products of the S_3 state of the oxygen-evolving complex of Photosystem II at cryogenic temperatures. Pathways to the formation of the $S=7/2$ S_2 state configuration, Biochemistry 41 (2002) 9580–9588.
[50] D.J. MacLachlan, J.H.A. Nugent, Investigation of the S_3 electron paramagnetic resonance signal from the oxygen-evolving complex of Photosystem 2: effect of inhibition of oxygen evolution by acetate, Biochemistry 32 (1993) 9772–9780.
[51] V. Szalai, H. Kühne, K.V. Lakshmi, G.W. Brudvig, Characterization of the interaction between manganese and tyrosine Z in acetate-inhibited Photosystem II, Biochemistry 37 (1998) 13594–13603.
[52] V. Petrouleas, D. Koulougliotis, N. Ioannidis, Trapping of metalloradical intermediates of the S-states at liquid helium temperatures. Overview of the phenomenology and mechanistic implications, Biochemistry 44 (2005) 6723–6728.